Research paper

1,4-Cyclohexanedicarboxylato-bridged cobalt coordination polymers: Synthesis, crystal structures and magnetic properties

Luis D. Rosales-Vázquez [a], Víctor Sánchez-Mendieta [a,b,*], Iván García-Orozco [a], Susana Hernández-López [a], Diego Martínez-Otero [b], Raúl A. Morales-Luckie [b], Roberto Escudero [c], Francisco Morales [c]

[a] Facultad de Química, Universidad Autónoma del Estado de México, Paseo Colón y Paseo Tollocan, Toluca, Estado de Mexico 50120, Mexico
[b] Centro Conjunto de Investigación en Química Sustentable UAEM-UNAM, Carretera Toluca-Ixtlahuaca km. 14.5, Tlachaloya, Toluca, Estado de Mexico, Mexico
[c] Instituto de Investigaciones en Materiales, Universidad Nacional Autónoma de México, Apartado Postal 70-360, Ciudad de Mexico 04510, Mexico

ABSTRACT

Three coordination polymers have been synthesized, using self-assembly solution reactions at ambient conditions, combining Co(II) ion with 1,4-ciclohexanedicarboxylic acid, in the presence of 1,10-phenantrolione and two different 2,2′-bipyridines, as co-ligands: $[Co(H_2O)(cdc)(phen)]_n$ (**1**); $\{[Co(H_2O)(cdc)(4dmb)]\cdot 2H_2O\}_n$ (**2**); $\{[Co(H_2O)(cdc)(5dmb)]\cdot 3H_2O\}_n$ (**3**), where cdc = *e,a-cis*-1,4-ciclohexanedicarboxylato, phen = 1,10-phenantroline, 4dmb = 4,4′-dimethyl-2,2′-bipyridine, and 5dmb = 5,5′-dimethyl-2,2′-bipyridine. Crystallographic studies show that these compounds have one-dimensional (1D) structures; Co(II) in **1**–**3** is six-coordinated with a distorted-octahedral coordination sphere. Complexes **2** and **3** exhibit a novel bridging motif of the cdc ligand in its *equatorial, axial cis* configuration. In addition, the solid-state self-assembly of the polymeric structure of **1** gives rise to a 2D supramolecular framework, mainly through hydrogen bonding. In contrast, complex **2** forms an infinite 1D supramolecular array, made of double Co ion rows bridged by hydrogen bonding interactions. Complex **3** generates an intricate 2D supramolecular framework also throughout hydrogen bonding. The thermal stabilities of the three coordination polymers were investigated. Magnetic properties measurements reveal that complexes **1**–**3** exhibit weak antiferromagnetic ordering with $\theta_{(C-W)}$ = −9.6, −5.8 and −7.5 K, and E_2 = 0.51, 0.16 and 0.28 cm^{-1}, accordingly to Curie-Weiss model and Rueff phenomenological approach, respectively.

1. Introduction

The design of hybrid metal-organic polymeric and supramolecular architectures, based on crystal engineering, has gained substantial interest in recent years in coordination chemistry, supramolecular chemistry and materials science, since these structures can acquire fascinating arrays and work as functional materials [1]. Crystal engineering refers to the construction of crystal structures from organic and metal-organic compounds using design principles that come from an understanding of the intermolecular interactions in the molecular solids [2]. Several strategies have been developed to synthesize metal mixed ligands coordination polymers of bivalent transition metals containing nitrogen and oxygen donor ligands [3]. Self-assembly of small molecules, compounds or complexes, proved to be a valuable pro-

cedure for the synthesis of large structures with a minimum of effort. However, the self-assembly process is sometimes accompanied by an uncertainty halo, due to unpredictable interactions among metal centers and ligands, especially when weak forces (e.g. hydrogen bonding, π-π interactions) and/or solvents, such as water, are involved [4]. Also, supramolecular frameworks based on metal centers and organic ligands have gained interest recently, due to their fascinating structural diversity and their potential applications in catalysis, sensing, porosity and non-linear optics [5]. Among the most used bridging ligands for transition metals are the dicarboxylates [6]. Perhaps the main reason to keep investigating the dicarboxylates as bridging ligands of metal centers, is the, at times, surprising variety of coordination modes that these organic compounds can accomplish, yielding thus interesting extended metal-organic molecular and supramolecular structures possessing divergent dimensionalities and properties [7]. Coordination polymers having cdc as bridging ligand have been prepared, though no so extensive; moreover, most of those compounds have been synthesized using solvothermal or hydrothermal methods [8]. The use of 2,2′-bipyridine as an ancillary ligand had become

* Corresponding author at: Facultad de Química, Universidad Autónoma del Estado de México, Paseo Colón y Paseo Tollocan, Toluca, Estado de Mexico 50120, Mexico.
E-mail address: vsanchezm@uaemex.mx (V. Sánchez-Mendieta).

relevant in our previous studies on complexes [9] and coordination polymers [10] of different metals. Therefore, we decided to continue with one of the most studied nitrogen donor ligands [11], but varying its alkyl substituent, in order to verify the influence of the co-ligand on the dimensionalities and crystalline structures of the resulting coordination polymers. So far, few articles have been published on the use of different di-alkyl-2,2′-bipyridines as ancillary ligands, either in transition metal complexes [12] or coordination polymers [13,14].

In this article, we describe the synthesis, crystalline molecular and supramolecular structures, thermal analyses and magnetic properties of three coordination polymers of three coordination polymers of formulae $[Co(H_2O)(cdc)(phen)]_n$ (**1**), $\{[Co(H_2O)(cdc)(4dmb)]\cdot 2H_2O\}_n$ (**2**) and $\{[Co(H_2O)(cdc)(5dmb)]\cdot 3H_2O\}_n$ (**3**) (cdc = *e,a-cis*-1,4-ciclohexanedicarboxylato, phen = 1,10-phenantroline, 4dmb = 4,4′-dimethyl-2,2′-bipyridine, and 5dmb = 5,5′-dimethyl-2,2′-bipyridine).

2. Experimental section

2.1. General considerations

All chemicals were of analytical grade, purchased commercially (Aldrich) and used without further purification. All syntheses were carried out under aerobic and ambient conditions. Elemental analyses for C, H, N were obtained by standard methods using a Vario Micro-Cube analyzer. IR spectra of the complexes were determined in a FT-IR Shimadzu spectrophotometer, IR Prestige-21, from 4000 to 500 cm^{-1}. Thermogravimetric analyses were performed in a SDT Q600 TA Instruments analyzer, under N_2 atmosphere, at a heating rate of 10 °C min^{-1}, from 20 to 700 °C. Magnetic characteristics of the complexes were determined with a MPMS Quantum Design magnetometer, with measurements performed at zero field cooling (ZFC) and field cooling (FC) from 2 to 300 K and decreasing. The applied magnetic field was 1000 Oe, and diamagnetic corrections were estimated using Pascal's constants as -250×10^{-6} cm^{3}mol^{-1}.

2.2. Preparation of $[Co(H_2O)(cdc)(phen)]_n$ (**1**)

Initially, sodium 1,4-cyclohexanedicarboxylate was prepared by adding an aqueous solution of NaOH (5 mL; 0.16 M) to a methanol solution (5 mL) of 1,4-cyclohexanedicarboxylic acid (0.0688 g; 0.4 mmol). A solution of 1,10-phenantroline (0.0744 g; 0.4 mmol) in methanol (5 mL) was added to the solution of sodium 1,4-cyclohexanedicarboxylate while stirring. Then, a de-ionized water solution (10 mL) of $Co(NO_3)_2\cdot 6H_2O$ (0.1164 g; 0.4 mmol) was added. A red-brown translucent solution was obtained. After five days, purple-brown crystals were achieved; these were filtered out and washed with de-ionized water. Yield: 49% based on metal precursor. Elemental analysis (%), $C_{20}H_{20}N_2O_5Co$, cal.: C, 56.21; H, 4.71; N, 6.55; found: C, 56.25; H, 4.64; N, 6.50. IR cm^{-1} (ATR): 3228 (m, br), 2924 (m), 1554 (s), 1516 (m), 1427 (m), 1404 (m), 1203 (s), 1146 (s), 964 (s), 910 (s), 841 (m, sh), 725 (m, sh), 671 (m, sh).

2.3. Preparation of $\{[Co(H_2O)(cdc)(4dmb)]\cdot 2H_2O\}_n$ (**2**)

Comparable conditions as in the synthesis of **1** were used, except that a solution of 4,4-dimetil-2,2′-bipyridine (0.0720 g; 0.4 mmol) in methanol (10 mL) was added to the solution of sodium 1,4-cyclohexanedicarboxylate while stirring. Yield: 43% based on metal precursor. Elemental analysis (%), $C_{20}H_{28}N_2O_7Co$, cal.: C, 51.39; H, 6.03; N, 5.99; found: C, 51.06; H, 6.02; N, 6.03. IR cm^{-1} (ATR): 3259 (m, br), 2943 (w), 1616 (m, sh), 1538 (s), 1512 (m), 1457 (m, sh), 1409 (s), 1014 (w, sh), 914 (m), 829 (m, sh), 767 (m, sh).

2.4. Preparation of $\{[Co(H_2O)(cdc)(5dmb)]\cdot 3H_2O\}_n$ (**3**)

Similar conditions as in the synthesis of **1** were used, except that a solution of 5,5′-dimethyl-2,2′-bpyridina (0.0720 g; 0.4 mmol) in methanol (10 mL) was added to the solution of sodium 1,4-cyclohexanedicarboxylate. Yield: 64% based on metal precursor. Elemental analysis (%), $C_{20}H_{30}N_2O_8Co$, cal.: C, 49.49; H, 6.23, N, 5.77; found: C, 50.02; H, 6.05; N, 5.58. IR cm^{-1} (ATR): 3420 (w, br), 2940 (w, sh), 1527 (s), 1470 (m, sh), 1427 (m, sh), 1404 (s, sh), 1349 (m, sh), 1254 (m, sh), 1144 (w, sh), 1044 (m, sh), 902 (w, sh), 841 (m, sh), 757 (m, sh), 687 (m, sh), 587 (m, sh).

3. X-ray crystallography

Crystallographic data for **1**–**3** were collected on a Bruker APEX II CCD Diffractometer, for **1** and **2** at 100 K and for **3** at 296 K, using Mo-Kα radiation (k = 0.71,073 Å) from an Incoatec IμS source and Helios optic monochromator [15]. Suitable crystals were coated with hydrocarbon oil (Parabar), picked up with a nylon loop, and mounted in the cold nitrogen stream of the diffractometer. The structures were solved using intrinsic phasing (SHELXT) [16] and refined by full-matrix least-squares on F^2 [16] using the shelXle GUI [17]. The hydrogen atoms of the C—H bonds were placed in idealized positions whereas the hydrogen atoms from water molecules were localized from the difference electron density map, and their position was refined with U_{iso} tied to the parent atom with distance restraints. In compound **2**, the hydrogens from water molecules that are not coordinated to cobalt present positional disorder in two positions, the occupation was set at 50% and their position were localized from the difference electron density map and refined using DFIX instruction. The hydrogens for methyl group (C11) present positional disorder in two positions that was solved using AFIX 123 constraint to fix the positions of hydrogens and the occupancy was fixed in 50%. The crystallographic data and refinement details for the polymers are summarized in Table S1. Selected bond lengths, angles and hydrogen bonding interactions for **1**–**3** are listed in Tables S2, S3 and S4, respectively.

4. Results and discussion

4.1. Synthesis and IR spectra

Using a very simple methodology of self-assembling solution reactions, equivalent amounts of 1,4-cyclohexanedicarboxylic acid, $Co(NO_3)_2$, and 1,10-phenantroline, 4,4′-dimethyl-2,2′-bipyridine and 5,5′-dimethyl-2,2′-bipyridine, respectively, were mixed in water-methanol solutions under ambient conditions. Slow evaporation of solvents yielded reddish-brown crystals of complexes **1**–**3**. These crystals are insoluble in common solvents.The IR spectra of the complexes show the typical bands (*vide supra*) expected for carboxylate ligands coordinated to Co(II) [18,19], along to the bands corresponding to the auxiliary ligands (Figs. S1–S3). Since the cdc bridging ligand has the same coordination modes in polymers **1**–**3**, relatively few variances can be observed in the IR spectra of these complexes. These IR spectra show two sets of asymmetric stretches for the carboxylate moiety at 1554 and 1516 cm^{-1}, 1538 and 1512 cm^{-1}, 1527 and 1470 cm^{-1}, with the corresponding symmetric stretches at 1404 and 1427 cm^{-1}, 1409 and 1457, 1404 and 1427 for **1**–**3**, respectively. The differences between asymmetric and symmetric stretch for the carboxylate ion (Δv^-_{COO}, cm^{-1}) are 150 and 89, 129 and 55, and 123 and 43, for **1**–**3**, respectively. These sets of bands can be assigned, correspondingly, to the bidentate chelate and monodentate coordination modes of the cdc ligand found in these complexes [20].

4.2. Structural description of [Co(H₂O)(cdc)(phen)]ₙ (**1**)

1 crystallizes in a monoclinic system with *P*2**₁**/*c* space group and forms an infinite one dimensional (1D) coordination polymer (Fig. 1). In fact, a complex almost identical to polymer **1** has been reported previously and its structural characterization has been analyzed [21]. However, that isostructural compound, with a different empirical formula, was obtained under hydrothermal conditions (about 180 °C for 6 days), whereas we synthesize the same compound at ambient conditions, using a very simple methodology; and, besides thermogravimetric analysis, no further properties were reported [21]. The repeat molecular unit of **1** contains one Co center, one cdc ligand, one phen co-ligand and one coordinated water ligand. The coordination environment of the Co is shown in Fig. S4a; the metal is six-coordinated and surrounded by four oxygen atoms from two different cdc ligands and the aqua ligand, and two nitrogen atoms from one phen ligand. The Co has a

distorted octahedral configuration. The Co-O bond lengths range from 2.0502(12) to 2.1774(12) Å, while the Co-N distances are 2.1100(14) and 2.1370(14) Å, these values are comparable to those found on similar Co(II) compounds [22–24]. In complex **1**, a 1D zig-zag chain is formed due to the combined monodentate η^1 and chelate bidentate η^2 coordination modes of cdc, together with the *equatorial, axial cis* configuration of its carboxylate groups, thus bridging the Co ions (Fig. S4b). Intermolecular hydrogen-bonding interactions assemble complex **1** into a 2D supramolecular array. These interactions are promoted mainly by the presence of the aqua ligand and the non-coordinated oxygen atom of the cdc carboxylate. This is shown in Fig. S4c, where the main O—H...O interactions involve the O—H moiety (O5) of the aqua ligand with each oxygen atom (O2) of the non-coordinated side of one cdc ligand, in an intramolecular hydrogen bond. Furthermore, each water ligand (O5) generates a double hydrogen bridge; the one described above, and another with one cdc oxygen atom (O3) coordinated to Co(II) of a neighboring 1D polymeric chain (intermolecular hydrogen bonding). In this way, an extended 2D supramolecular array is generated (Fig. S4c), in which, the intermolecular shortest Co...Co distance is 5.431 Å.

4.3. Structural description of {[Co(H₂O)(cdc)(4dmb)]·2H₂O}ₙ (**2**)

2 crystallizes in a monoclinic system with *P*2**₁**/*c* space group and forms an infinite 1D coordination polymer. The asymmetric unit contains one Co(II) ion, one cdc ligand, one 4dmb co-ligand, one aqua ligand and other two free water molecules. The coordination environment of the Co is shown in Fig. 1a; the metal center is six-coordinated and surrounded by four oxygen atoms from two different cdc ligands and the aqua ligand, and two nitrogen atoms from one 4dmb ligand. As in **1**, the Co ion has a distorted octahedral configuration. The Co-O bond lengths range from 2.0547(10) to 2.18,711(10) Å, while the Co-N distances are 2.0867(12) and 2.1377(12) Å, these values are like those found on related Co(II) compounds [25]. In complex **2**, a 1D chain is formed due to the combined monodentate η^1 and chelate bidentate η^2 coordination modes of cdc, along with the *equatorial, axial cis* configuration of its carboxylate groups bridging the metal centers (Fig. 1b). The way all Co ions align to one side of the 1D chain, with the cdc ligand completing a V-shaped "repeat unit" (Fig. 2b), is a new motif found in coordination polymers bearing the cdc bridging ligand. T.F. Liu, et al., have reported most of the motifs originated for this cdc ligand, in both, *trans* and *cis* conformations, while forming coordination polymers [26]. Thus, this type of novel motif has not been noticed neither in the *equatorial, axial cis* nor in the *equatorial, equatorial trans* conformations of cdc bridging ligand. There is only one report of a similar motif in a Cu(II) coordination polymer built on cdc and phenantroline [27]; nonetheless, authors did not comment on the cdc motif obtained.

Hydrogen-bonding interactions assemble complex **2** into a 1D supramolecular array with two-row of Co centers (Fig. 1c). These bindings are carried out by the presence of two molecules of water in the crystal, and their interactions with the aqua ligand and coordinated and non-coordinated oxygen atoms of the cdc ligand. This is shown in Fig. 2c, where the main O—H...O interactions involve the O—H moiety (O1) of the aqua ligand with each oxygen atom (O3) of the non-coordinated side of one cdc ligand, in an intramolecular hydrogen bond. Then, each water ligand (O1) generates a double hydrogen bridge; the one described above, and another with one water of crystallization (O7), which, in turn, bridges also with the other water of crystallization (O6) and with the non-coordinated side of the cdc ligand (O3) (intermolecular hydrogen bonding). In addition, the coordinated side of the cdc ligand (O5) makes also a hydrogen bridge with one water of crystallization (O6). These hydrogen-bonding fused rings cause the
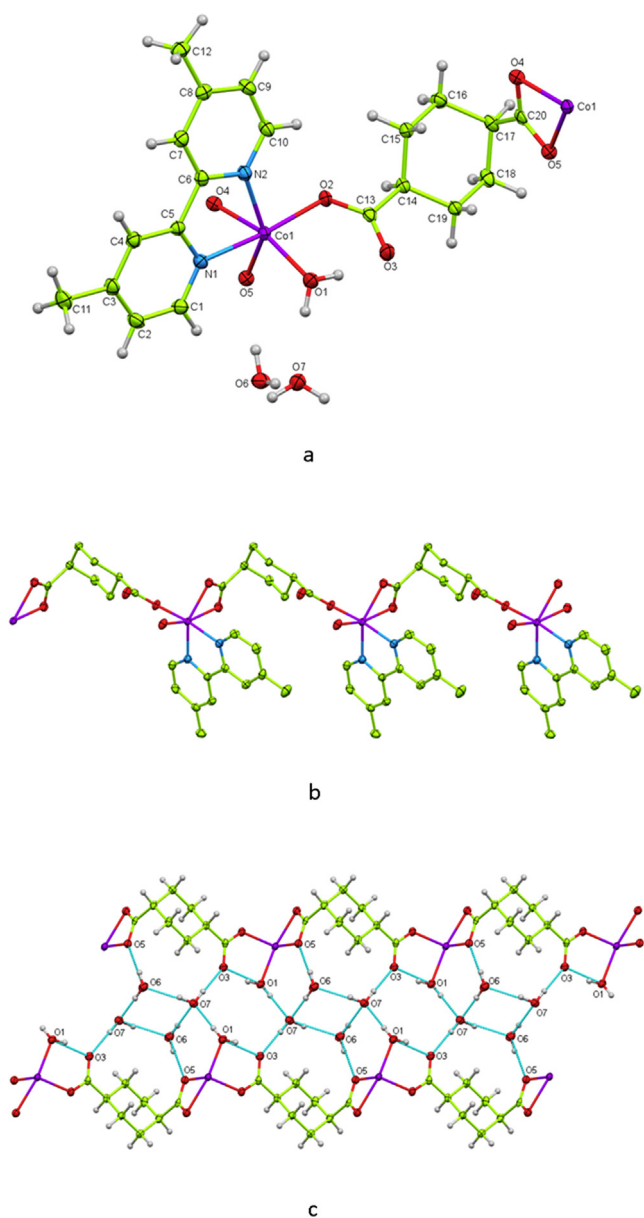

Fig. 1. Molecular structure of {[Co(H₂O)(cdc)(4dmb)]·2H₂O}ₙ (**2**) (ellipsoids shown at 60% probability) (a); 1D V-shape polymer chain of **2**; hydrogens are omitted for clarity (b); 1D supramolecular array in **2**; 4dmb ligand is omitted for clarity (c).
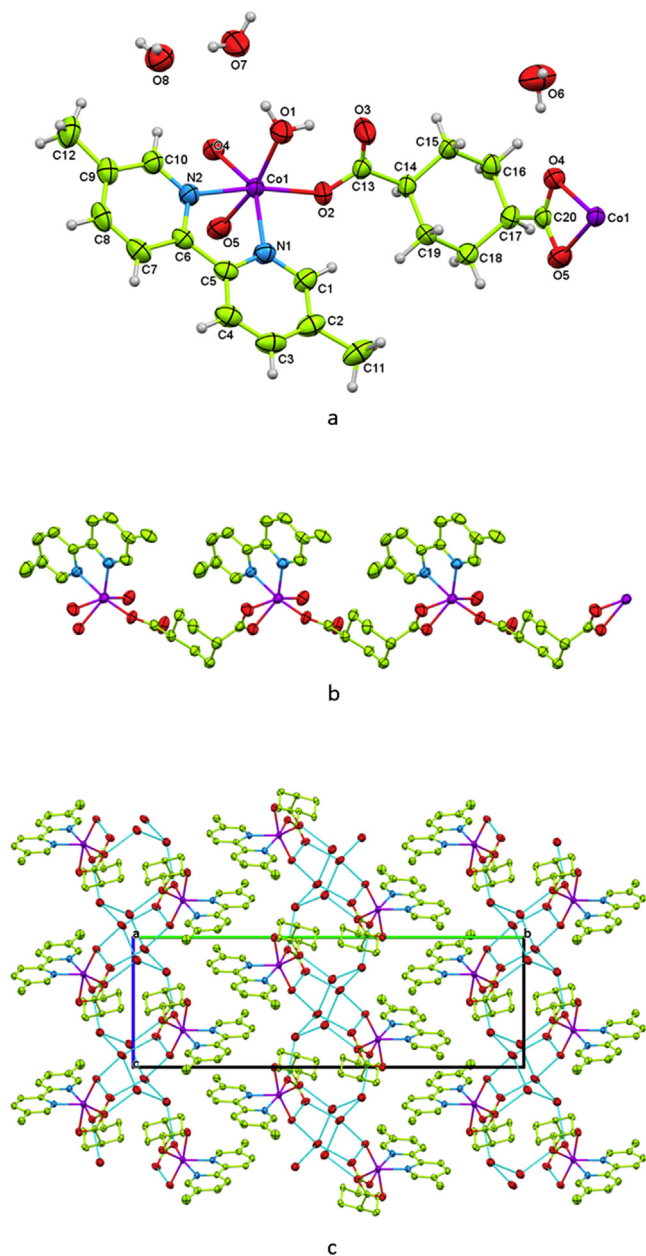
Fig. 2. Molecular structure of {[Co(H₂O)(cdc)(5dmb)]·3H₂O}ₙ (**3**) (ellipsoids shown at 60% probability) (a); 1D V-shape polymer chain of **3**; hydrogens are omitted for clarity (b); 2D supramolecular array in **3**; 5dmb ligand is omitted for clarity (c).

merger of two 1D polymeric chains, giving rise to a two-row Co 1D supramolecular system (Fig. 1c, Fig. S5).

4.4. Structural description of {[Co(H₂O)(cdc)(5dmb)]·3H₂O}ₙ (3)

3 crystallizes also in a monoclinic system with $P2_1/c$ space group and forms an infinite 1D coordination polymer. The asymmetric unit contains one Co(II) ion, one cdc ligand, one 5dmb co-ligand, one aqua ligand and other three free water molecules. The coordination environment of the Co is shown in Fig. 2a; the metal center is six-coordinated and surrounded by four oxygen atoms from two different cdc ligands and the aqua ligand, and two nitrogen atoms from one 5dmb ligand. As in **2**, the Co ion has a distorted octahedral configuration. The Co-O bond lengths range from 2.0634(13) to 2.2118(13) Å, while the Co-N distances are 2.0959(14) and 2.1622(13) Å; these values are similar to those

found on comparable Co(II) compounds [21–25]. In complex **3**, alike **2**, a 1D chain is formed owing to the combined monodentate η^1 and chelate bidentate η^2 coordination modes of cdc, beside with the *equatorial, axial cis* configuration of its carboxylate groups bridging the metal centers (Fig. 2b). Analogous to complex **2**, in the extended structure of **3** the Co metal centers align to one side of the 1D chain, with the cdc ligand forming a kind of V-shaped "repeat unit" (Fig. 2b), which, as mentioned before, is a new motif found in coordination polymers having cdc as bridging ligand [26]

Hydrogen bond interactions gather complex **3** into a 2D supramolecular array (Fig. 2c). These bindings are formed by the presence of three molecules of water in the crystal, and their interactions with the aqua ligand and the coordinated and non-coordinated oxygen atoms of the cdc ligand. Similarly to complex **2**, the main O—H⋯O interactions involve the O—H moiety (O1) of the aqua ligand with each oxygen atom (O3) of the non-coordinated side of one cdc ligand, in an intramolecular hydrogen bond. Also, each aqua ligand (O5) generates a double hydrogen bridge; the one defined above, and another with one water of crystallization (O7), which, consecutively, bridges also with the two other water of crystallization molecules (O6 and O8) and non-coordinated side of the cdc ligand (O3) (intermolecular hydrogen bonding). Furthermore, the coordinated side of the cdc ligand (O4) creates also a hydrogen bridge with one water of crystallization (O6), and this latter makes a bridge also with another water of crystallization (O8). These elaborate hydrogen bonding array in **3** provokes the formation of six-member fused rings (without including the hydrogen atoms), causing the merger of 1D polymeric chains and generating a chain links type system (Fig. 2c), which grows in the *a* crystallographic axis giving rise thus to a 2D supramolecular system (Fig. S6).

4.5. Thermal properties of 1–3

To examine the thermal stabilities of the crystalline polymers, thermal analyses were performed for the complexes between 20 and 700 °C (Figure S7). The TGA plots for the three complexes can be analyzed as having three main stages of decomposition. The first weight loss (5.0%) for **1** occurs between 170 and 212 °C; the second, with a weight loss of 7.0% of the initial weight, takes place approximately between 246 and 339 °C. The final weight loss (44%) occurs around 342–516 °C. For complex **2**, the first weight loss (∼9%) appears between 76 and 157 °C. The second loss (17%) starts around 179 °C and ends at 273 °C. The final loss (∼58%) occurs from 290 to 495 C, leaving around 14% of the initial sample weight at 700 °C. In complex **3**, the first weight loss (10%) occurs between 70 and 127 °C; the second, with a weight loss of 36.0% of the initial weight, takes place approximately between 286 and 377 °C; and the final weight loss (∼33%) occurs around 384–483 °C, leaving around 15% of the initial sample weight at 700 °C. In these three complexes, the first decomposition stages can be ascribed to the loss of water; however, for complex **1** one coordinated water ligands is lost, whilst for complexes **2** and **3**, two and three molecules of water of crystallization are lost, respectively. Additionally, these latter complexes also lost one aqua ligand each. The higher-temperature stages can be attributed to the combined weight loss of the cdc ligand (calcd. 39% for **1**, 36% for **2** and 35% for **3**), and the phen (calcd. 42%), 4dmb (calcd. 39%) and 5dmb (calcd. 38%) co-ligands, respectively. The residual material, at 700 °C, for complexes **2** and **3**, approximates to residual CoO (calcd. 16% for **2** and 15% for **3**). It is evident that due to their different structural characteristics, mainly supramolecular, polymer **1** has superior thermal stability compared to those of **2** and **3** (Fig. S7); so, the residual weight for **1** at 700 °C is approximately 40%.

4.6. Magnetic properties of **1–3**

The calculated magnetic susceptibility (χ_M), in terms of $cm^3 mol^{-1}$, vs. temperature for **1–3**, can be seen in Figs. 3–5. Although no maximum is observed in the susceptibility plots, the observed increase of χ_M, and the decrease in χT (Figs. S8–S10), with decreasing temperature, suggests antiferromagnetic coupling, albeit very weak. After fitting the obtained data to Curie-Weiss model:

$$\chi_M = C/(T - \theta) \tag{1}$$

The Curie constants were determined to be, C = 2.76, 2.85 and 2.51 cm^3 K/mol for **1–3**, respectively; S = 3/2, with a small orbital contribution, not totally quenched, and influences to a value of orbital angular contribution less than one. The Curie-Weiss temperatures were determined to be $\theta_{(C-W)}$ = −9.64, −5.83 and −7.53 K for **1–3**, respectively, indicative of an antiferromagnetic ordering. Regularly, the effects of spin–orbit coupling occur in combination with the effects of a symmetry-lowering structural distortion, for instance away from O_h symmetry [28], as it is the case for complexes **1–3**. From the χT values obtained at 300 K, a μ_{eff} = 4.7, 4.8 and 4.5 μ_B are calculated for **1–3**, respectively, which are higher than the expected spin-only value of 3.87 μ_B corresponding to three unpaired electrons for high-spin d^7-Co^{2+}; however, the obtained value agrees with those reported in literature for high-spin Co(II) complexes [29] and confirms an S = 3/2 spin state. These results are in concordance with previous magnetic studies carried out on a Co(II) complex containing 3,6-ditert-butyl-o-benzosemiquinonato ligands and 5,7-di-*tert*-butyl-2-(pyridine-2-yl) benzoxazole having distorted octahedral geometry [30]. However, as observed in Figs. 3–5, it was difficult to fit the Curie-Weiss model to the χ_M vs. T plot, particularly below 25 K. Therefore, assuming that in the low-temperature region the spin-orbit coupling is promoted in these systems, the magnetic exchange interactions and the spin–orbit coupling for complexes **1–3** were also estimated based on the simple phenomenological equation:

$$\chi_M T = A\exp(-E_1/kT) + B\exp(-E_2/kT) \tag{2}$$

where $A + B$ is equal to the Curie constant and E_1 and E_2 are the "activation energies" of the spin–orbit coupling and the magnetic interaction, respectively [31]. As shown in Figs. 3–5, for the χ_M vs. T plot, Rueff model [32] follows very well the experimental data, even at the lowest temperature studied (Figs. 3–5; Figs. S8–S10). The best parameters obtained with this procedure after least-squares fitting are: $A + B$ = 2.90, 3.01 and 2.59 cm^3·K·mol^{-1} for **1–3**, respectively, which agree with values given in the literature for the Curie constant

Fig. 3. χ_M vs. T plot for **1**.
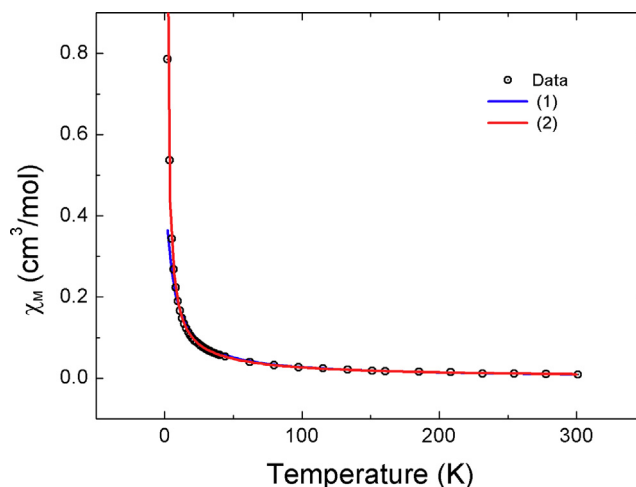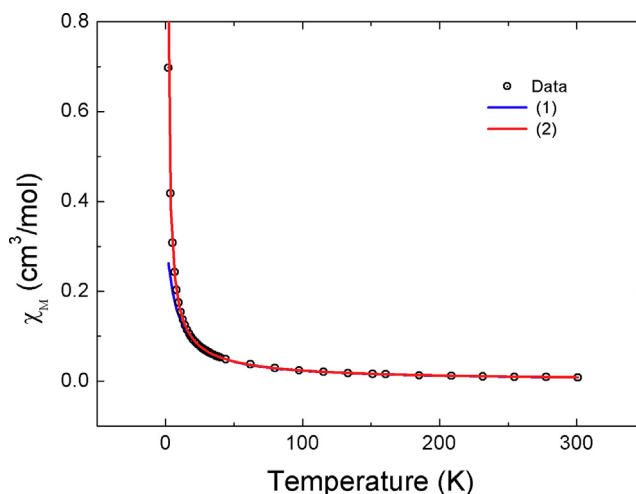

Fig. 4. χ_M vs. T plot for **2**.

Fig. 5. χ_M vs. T plot for **3**.

(C = 2.8 – 3.5 emu·K·mol^{-1}), and also practically equals the values obtained from the fitting of Curie-Weiss model showed previously. The effect of the spin–orbit coupling E_1 = 38.45, 37.96 and 28.32 cm^{-1} for **1–3**, respectively, are lower than values reported for other Co(II) systems (52 to 65 cm^{-1}) [31,32], which, by the way, are not supramolecular systems but rather are extended coordinated compounds. The positive, and low, values of activation energy E_2 = 0.51, 0.16 and 0.28 cm^{-1} for **1–3**, respectively, confirms that antiferromagnetic exchanges are effective in these polymers and also that these interactions are weak. These E_1 and E_2 values obtained for **1–3** are very similar to those found in a Co(II)-fumarato complex, having a rare distorted-trigonal prismatic geometry, which also has hydrogen bonding interactions yielding a 2D supramolecular structure [33]. Hence, regarding the fitting of Eq. (2) to these divergent systems, it seems that the difference in coordination geometry does not influence significantly the Co(II) spin–orbit coupling and the magnetic interaction (E1 and E2 values), but rather are the distances among metal ions in the supramolecular arrays the important factor; therefore, in the Co(II) coordination complex reported in reference 33 and complex **1** from this work, the distances between metal centers are comparable: 6.143 and 5.43 Å, respectively. Accordingly to the $\theta_{(C-W)}$ and E_2 values of the three polymers, complex **1** possesses the less weak antiferromagnetic exchange. This situation could be explained by the different magnetic exchange pathways occurring in these complexes. In polymer **1** the main magnetic exchange

corridor appears to be the strong hydrogen binding interactions occurring through the connections involving the coordinated water (O5) and one of the oxygen atoms (O3) in the carboxylate moiety of cdc ligand, belonging to a neighboring 1D complex molecule, [Co-O5-H5B—O3-Co] (Fig. S4c). Thus, these interactions produce the shortest Co—Co distance of 5.43 Å in the supramolecular structure of **1**; on the other hand, in complexes **2** and **3** the shortest Co—Co distances are 8.84 and 8.22 Å, respectively. In these latter complexes, the hydrogen-bonding interactions (Figs. 1c and 2c) do not cause an approaching effect of metal ions in the corresponding supramolecular structures, as it occurs in **1**. Hence, the shorter the distance between metal centers the larger is the corresponding E_2 value.

5. Conclusions

We have reported the synthesis and characterization of three crystalline Co(II) coordination polymers formed with 1,4-cyclohexanedicarboxylato and different 2,2′-bipyridine type co-ligands *via* self-assembly reactions. In complexes **1**–**3**, the bridging cdc ligand coordination modes are monodentate η^1 and chelate bidentate η^2; these compounds have one-dimensional (1D) structures, where the Co metal centers are six-coordinated with a distorted-octahedral coordination sphere. Complexes **2** and **3** display a new bridging motif of the cdc ligand in its *equatorial, axial cis* configuration. Furthermore, the solid-state assemblies of the polymeric structures of **1**–**3** generate supramolecular frameworks, mainly through hydrogen bonding: 2D for complexes **1** and **3**, and 1D for complex **2**. The positive and low values for E_2 (Rueff phenomenological model) and the negative, and also low, values of $\theta_{(C-W)}$ (Curie-Weiss model), obtained in all three polymers, reveal weak antiferromagnetic exchange in these Co(II) systems.

Acknowledgments

Appendix A. Supplementary data

Supplementary data associated with this article can be found, in the online version, at https://doi.org/10.1016/j.ica.2017.12.007.

References

[1] (a) R. Robson, Dalton Trans. (2008) 5113;
(b) C. Yamamoto, H. Nishikawa, M. Nihei, T. Shiga, M. Hedo, Y. Uwatoko, H. Sawa, H. Kitagawa, Y. Taguchi, Y. Iwasa, H. Oshio, Inorg. Chem. 45 (2006) 10270;
(c) H.C. Zhou, J.R. Long, O.M. Yaghi, Chem. Rev. 112 (2012) 673.
[2] G.R. Desiraju, J.J. Vittal, A. Ramanan, Crystal Engineering-A Text Book, IISc Press and World Scientific, Singapore, 2011.
[3] M. Dua, C.-P. Li, C.-S. Liub, S.-M. Fang, Coord. Chem. Rev. 257 (2013) 1282.
[4] D. Das, R. Banerjee, R. Mondal, J.A.K. Howard, R. Boese, G.R. Desiraju, Chem. Commun. (2006) 555.
[5] X.H. Zhou, L. Li, H.H. Li, A. Li, T. Yang, W. Huang, Dalton Trans. 42 (2013) 12403.
[6] D. Curiel, M. Más-Montoya, G. Sánchez, Coord. Chem. Rev. 284 (2014) 19.
[7] B.-H. Ye, M.-L. Tong, X.-M. Chen, Coord. Chem. Rev. 249 (2005) 545.
[8] D. Sun, M.-Z. Xu, S.-S. Liu, S. Yuan, H.-F. Lu, S.-Y. Feng, D.-F. Sun, Dalton Trans. 42 (2013) 12324.
[9] A. Téllez-López, V. Sánchez-Mendieta, J. Jaramillo-García, L.D. Rosales-Vázquez, I. García-Orozco, R.A. Morales-Luckie, R. Escudero, F. Morales-Leal, Transition Met. Chem. 41 (2016) 879.
[10] L.D. Rosales-Vázquez, V. Sánchez-Mendieta, A. Dorazco-Gonzalez, D. Martínez-Otero, I. García-Orozco, R.A. Morales-Luckie, J. Jaramillo-García, A. Tellez-Lopez, Dalton Trans. 46 (2017) 12516.
[11] R.D. Hancock, Chem. Soc. Rev. 42 (2013) 1500.
[12] R. Alizadeh, V. Amani, Inorg. Chim. Acta 443 (2016) 151.
[13] L.B. Lopes, C.C. Corrêa, G.P. Guedes, M.G.F. Vaz, R. Diniz, F.C. Machado, Polyhedron 50 (2013) 16.
[14] G.M. Zhang, Y. Li, X.Z. Zou, J.A. Zhang, J.Z. Gu, A.M. Kirillov, Transition Met. Chem. 41 (2016) 153.
[15] APEX 2 software suite, Bruker AXS Inc., Madison, Wisconsin, USA.
[16] G.M. Sheldrick, Acta Crystallogr. A 71 (2015) 3.
[17] C.B. Hübschle, G.M. Sheldrick, B. Dittrich, ShelXle, Appl. Cryst. 44 (2011) 1281.
[18] J. Do, Y. Lee, J. Kang, Y.S. Park, B. Lorenz, A.J. Jacobson, Inorg. Chem. 51 (2012) 3533.
[19] T.A. Beard, J.A. Wilson, R.L. LaDuca, Inorg. Chim. Acta 466 (2017) 30.
[20] C.C.R. Sutton, G. da Silva, G.V. Franks, Chem. Eur. J. 21 (2015) 6801.
[21] Y. Qi, Y. Wang, C. Hu, M. Cao, L. Mao, E. Wang, Inorg. Chem. 42 (2003) 8519.
[22] B.-J. Zhang, C.-J. Wang, G.-M. Qiu, S. Huang, X.-L. Zhou, J. Wenga, Y.-Y. Wang, Inorg. Chim. Acta 397 (2013) 48.
[23] J.-H. Guo, J. Chen, C.-P. Li, M. Du, J. Mol. Struct. 975 (2010) 147.
[24] Y. Xie, F.Y. Bai, J. Li, Y.H. Xing, Z. Wang, H.Y. Zhao, Z.F. Pu, M.F. Ge, Z. Shi, Spectrochimica Acta Part A 77 (2010) 749.
[25] X.-L. Wang, F.-F. Sui, H.-Y. Lin, J.-W. Zhang, G.-Ch. Liu, Cryst. Growth Des. 14 (2014) 3438.
[26] T.-F. Liu, J. Lü, R. Cao, Cryst. Eng. Comm. 12 (2010) 670.
[27] A.-Q. Ma, M.-X. Yu, L.-G. Zhu, Z. Kristallogr. NCS 219 (2004) 63.
[28] O. Kahn, Mol. Magn., VCH Publishers, New York, 1993.
[29] R.L. Carlin, Magnetochemistry, Springer-Verlag, Berlin, 1986.
[30] N.A. Protasenko, A.I. Poddel'sky, A.S. Bogomyakov, N.V. Somov, G.A. Abakumov, V.K. Cherkasov, Polyhedron 49 (2013) 239.
[31] P. Rabu, J.M. Rueff, Z.-L. Huang, S. Angelov, J. Souletie, M. Drillon, Polyhedron 20 (2001) 1677.
[32] (a) J.M. Rueff, N. Masciocchi, P. Rabu, A. Sironi, A. Skoulios, Eur. J. Inorg. Chem. (2001) 2843;
(b) J.M. Rueff, N. Masciocchi, P. Rabu, A. Sironi, A. Skoulios, Chem. Eur. J. 8 (2002) 1813.
[33] A. Téllez-López, J. Jaramillo-García, R. Martínez-Domínguez, R.A. Morales-Luckie, M.A. Camacho-López, R. Escudero, V. Sánchez-Mendieta, Polyhedron 100 (2015) 373.